PREDICTION OF THE UNIAXIAL TENSILE PLASTIC BEHAVIOR OF AN INTERSTITIAL FREE STEEL USING DIFFERENT WORK-HARDENING EQUATIONS *

Tiago Bristt Gonoring [1]
Marcos Tadeu D'Azeredo Orlando [2]
Jetson Lemos Ferreira [3]
Marden Valente de Souza [4]
Luciano Pessanha Moreira [5]

Abstract

The necessary time to launch a vehicle has been reduced year by year thanks to, among other factors, software improvement that can predict metal forming process and application performances. The material behavior is one of fundamental issue to guarantee accuracy in numerical simulations. The relationship of the stress-strain determined by uniaxial tensile test is an information required in forming software. The strains obtained in stamping process normally are higher than those reached by tensile test. Therefore, it is necessary to extrapolate of the tensile data to predict the steel plastic behavior under biaxial stress state. This implies the development of new work-hardening equations or better identification methods of classical equations. Among the models already known, this study makes use of the following work-hardening equations: Hollomon, Ludwik, Swift, Hockett-Sherby and Voce to describe the uniaxial tensile behavior of steel sheets. The results showed that the Swift, Hockett-Sherby and Voce equations, in general, present good fit to the experimental data. Both initial yielding and large straining domains of the stress-strain curve are better described by the Hockett-Sherby, and the combination of the Swift and Hockett-Sherby plastic models.

Keywords: Work-hardening models, Sheet Metal Forming, Numerical Simulation, Deep Drawing Quality Steel.

[1] *Doutorando, Me., Engenheiro Metalurgista, Programa de Pós-Graduação em Engenharia Mecânica, Universidade Federal do Espírito Santo, Vitória, Espírito Santo, Brasil.*
[2] *Professor Titular, Dr., Programa de Pós-Graduação em Engenharia Mecânica, Universidade Federal do Espírito Santo, Vitória, Espírito Santo, Brasil.*
[3] *Doutorando, Me., Engenheiro Metalurgista, Gerência do Centro de Pesquisa e Desenvolvimento da ArcelorMittal, Vitória, ES, Brasil e Universidade Federal Fluminense, Volta Redonda, RJ, Brasil.*
[4] *Me., Engenheiro Metalurgista, Gerência do Centro de Pesquisa e Desenvolvimento da ArcelorMittal, Vitória, ES, Brasil.*
[5] *Professor Associado, D.Sc., Universidade Federal Fluminense, Volta Redonda, RJ, Brasil.*

** Technical contribution to the 56º Seminário de Laminação e Conformação de Metais, part of the ABM Week 2019, October 1st-3rd, 2019, São Paulo, SP, Brazil.*

1 INTRODUCTION

In the automotive industry, a numerical simulation is an important step in order to optimize sheet metal forming processes, as well as a tool that enables detection and prevention of eventual failures, leading to a constant reduction of time, cost and improvement of the final product quality. These factors favor the reduction in time required to launch new vehicles on the market.

The numerical simulation accuracy will depend on steel's mechanical properties, which can be characterized by its strain hardening curve obtained in a uniaxial tensile test [1,2]. However, the extent of plastic strain achieved in a tensile test is much lower compared to other loading modes, and also to the large strain levels that are obtained for most metal forming processes [3]. Since numerical simulation needs to predict large strains, it is necessary to generalize the strain hardening curve to larger values of plastic straining.

The hydraulic bulge test, or biaxial bulge test, is an alternative method to evaluate the strain-hardening of steel sheets in the large strain domain [4]. This mechanical test is known for its ability to plastically deform materials to higher strain levels compared to the uniaxial tensile test, mainly due to the imposed biaxial stress state and friction absence between the blank specimen and the tools [4].

In addition to intrinsic strain hardening characteristics of the sheet material, mathematical models are used to describe mechanical behavior in sheet metal forming, that is, a plastic flow criterion and constitutive equation models are adopted. For each material, constitutive equations parameters can be obtained from uniaxial and equibiaxial stress curves [1].

The objective of this work is to perform a data conversion or data description from the symmetrical biaxial strain hardening curve, generated from the hydraulic bulge test, to the uniaxial strain and to propose which constitutive model best describes the mechanical forming behavior of the evaluated material.

2 MATERIALS AND METHODS

2.1 Uniaxial Tensile Test

Uniaxial tensile tests were performed on an Instron universal tensile machine and test specimens were made according to *sheet type* recommendations from ASTM A 370 standard [5]. The specimens were manufactured from a steel sheet, and obtained out from different directions at 0°, 45° and 90° relative to the rolling direction. Tensile tests were performed at room temperature at a constant strain rate of 0.001/s until rupture. Equations (1) and (2) were used for the uniaxial tensile test data to obtain the true stress-strain curve, which was plotted up to the tensile strength (TS).

$$\varepsilon = ln(1+e) = ln\left(1+\frac{\Delta l}{l_0}\right) \quad (1)$$

$$\sigma = \frac{F}{A_0}\cdot(1+e) = \frac{F}{A_0}\cdot\left(1+\frac{\Delta l}{l_0}\right) \quad (2)$$

Where F is the force (N) applied to the specimen and A_0 is the initial cross-section area (mm^2); l_0 is the initial length (mm) and Δl (mm) is the elongation relative to l_0 (mm) on the specimen. Curves will be adjusted according to rigid-plastic constitutive models proposed in the literature in addition to the experimental determination of the strain hardening curve.

2.2 Hydraulic Bulge Test

The hydraulic bulge test consists of fixing, by means of a high load (blank holder forces – F_{BH}), a thin, generally circular, sheet metal specimen of initial thickness t_0, which shall be subjected to a hydraulic pressure (P) according to the schematic drawing shown in Figure 1 [6]. The specimen is progressively deformed by the action of hydraulic pressure in the place of a punch, minimizing any frictional influence [1]. The fluid pressure against one side of

the sheet increases over time, deforming it and forming a protruding central region - hemispherical dome, whose material thickness at the pole (t) tends to decrease more intensely than at the peripheral region, while constant latitude circles are formed at the internal surface (hydraulic fluid and sheet surface contact). Under these conditions, a symmetrical biaxial state (stretch), with rotational symmetry, is generated on the pole [6, 7, 8]. As strain advances, this protuberance tends to present a smaller and smaller curvature radius (ρ), so, this curvature can be considered infinite at the beginning of the test, when the sheet is flat.

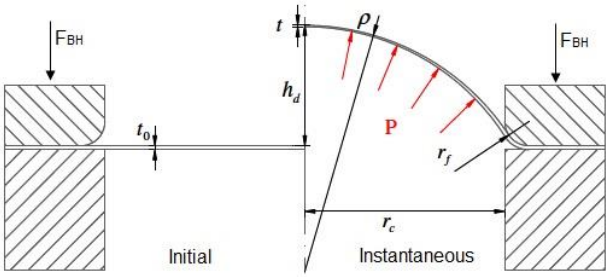

FIGURE 1. Schematic representation of a sheet hydraulic bulge test., Adapted from Maummer *et al* [6].

Hydraulic bulge tests were performed on a universal forming press, with blank holder force and press speed of 500 kN and 60 mm / min, respectively. The specimens used in the hydraulic bulge tests were circular with 180 mm in diameter. The hydraulic pressure (p), sheet thickness at the pole (t), and the curvature radius (ρ) are recorded during the hydraulic bulge test.

Values for pressure p were acquired directly from the forming press using a software. Values for the curvature radius of the specimen (ρ), hydraulic pressure (P), and instantaneous pole thickness (t) were also determined automatically. This software determines the radius (ρ), although the procedures for this calculation are not described.

2.2.1 Biaxial stress-strain curve definition

An analysis of the stress state in the vicinity of the hemispherical dome during the biaxial test is performed using equation (3), known as the stress equation for thin-walled pressure vessels, also known as membrane theory. [9].

$$\frac{\sigma_1}{\rho_1} + \frac{\sigma_2}{\rho_2} = \frac{P}{t} \qquad (3)$$

Where σ_1 and σ_2 are the principal stresses on the sheet surface (assuming that the main stresses axes -0123- and the anisotropic axes -0xyz- are coincident), ρ_1 and ρ_2 are the curvature radii in the middle of the sheet thickness (t), and p is the hydraulic pressure [1]. Since the ratio between sheet thickness and its diameter is less than 1/50, under these conditions bending stresses can be neglected and it is assumed that σ_3 equals zero [1].

On the other hand, the curvature radii are experimentally evaluated on the outer dome surface outer surface, then their adjustment can be performed using equation (4):

$$\rho = \rho_{ext} - \frac{t}{2} \qquad (4)$$

Where ρ is the curvature radius at half the thickness of the pole, and ρ_{ext} is the curvature radius of the hemispherical dome outer surface.

In equation (3), σ_1 and σ_2 are unknown and an additional equation is required for their determination. For anisotropic metals that meet the Hill's 48 yield criterion [10], equation (5) can be used, assuming that the main stress axes (0123) and the anisotropic axes (Oxyz) are coincident [1].

$$\left.\begin{aligned} d\varepsilon_1 &= d\lambda[(G+H)\sigma_1 - H\sigma_2], \\ d\varepsilon_2 &= d\lambda[(F+H)\sigma_2 - H\sigma_1] \end{aligned}\right\} \qquad (5)$$

Where F, G and H are anisotropic parameters, $d\varepsilon_1$ and $d\varepsilon_2$ are plastic strain increments in the sheet plane parallel to Ox and Oy axes, respectively, and dλ is a

scalar proportionality factor. Knowing F, G and H parameters from Hill's 48 criterion, it's possible to find out σ_1 and σ_2.

In order to determine F, G and H, the plastic anisotropy coefficients (r_α), relative to different angular orientations with respect to the rolling direction (α) at 0, 45 and 90º, are calculated from uniaxial tensile tests.

The relationships between Hill's 48 criterion parameters and anisotropy coefficients (r_α) are presented in equation (6) [11; 12]:

$$F = \frac{r_0}{r_{90}(1+r_0)} \quad , G = \frac{1}{1+r_0} \quad , \quad H = \frac{r_0}{1+r_0} \qquad (6)$$

The thickness strain ε_3 is obtained from the surface principal strains assuming plastic incompressibility, ε_1 and ε_2, as long as the material's volume remains constant during plastic strain [13] (equation (7)) :

$$\varepsilon_1+\varepsilon_2+\varepsilon_3 = 0 \qquad (7)$$

2.2.2 Biaxial and uniaxial Stress-Strain Transformation

Two distinct strain hardening curves to the same material can be obtained from uniaxial tensile and hydraulic bulge tests, where $\sigma_u = f(\varepsilon)$, that comes from the uniaxial tensile test and $\sigma_b = f(\varepsilon)$ that comes from the bulge test.

Since the curves do not come from the same strain mode, they cannot be directly compared, so a combination of data cannot be performed [14]. To perform the equibiaxial data description to uniaxial strain, it is necessary to calculate the equivalent stress and strain, that are $\bar{\sigma}$ and $\bar{\varepsilon}$, respectively, which represent this data description, from symmetrical biaxial strain hardening curve to uniaxial strain.

2.2.2.1 Hill's 48 and von Mises Equivalent Stress-strain

Equations (8) and (9) can be used to calculate the equivalent stress and strain, which are simplifications of the quadratic function from Hill'48 plastic flow criterion [8, 10, 13, 15]:

$$\bar{\sigma} = \sqrt{(G+H)\sigma_1^2 + (F+H)\sigma_2^2 - 2H\sigma_1\sigma_2} \qquad (8)$$

$$\bar{\varepsilon} = \sqrt{F\left[\frac{G\varepsilon_2 - H\varepsilon_3}{FG+GH+HF}\right]^2 + G\left[\frac{F\varepsilon_1 - H\varepsilon_3}{FG+GH+HF}\right]^2 + H\left[\frac{F\varepsilon_1 - G\varepsilon_2}{FG+GH+HF}\right]^2} \qquad (9)$$

Rana et al [7] applied the Hill'48 yield criterion to several classes of IF steels as described below in equations (10) and (11):

$$\bar{\sigma} = \sigma_1\sqrt{\frac{3}{2}\left(\frac{r_0+r_{90}}{r_0 r_{90}+r_0+r_{90}}\right)} \qquad (10)$$

$$\bar{\varepsilon} = |\varepsilon_3| \cdot \left\{\frac{3}{2}\left(\frac{r_0+r_{90}}{r_0 r_{90}+r_0+r_{90}}\right)\right\}^{-1/2} \qquad (11)$$

For isotropic materials that meet von Mises criterion (F = G = H = 0.5), equations (8) and (9) are reduced to equations (12) and (13) respectively.

$$\bar{\sigma} = \sqrt{\sigma_1^2 + \sigma_2^2 - \sigma_1\sigma_2} \qquad (12)$$

$$\bar{\varepsilon} = \left(\frac{2}{\sqrt{3}}\right)\sqrt{\varepsilon_1^2 + \varepsilon_2^2 + \varepsilon_1\varepsilon_2} \qquad (13)$$

In cases of completely isotropic or anisotropic materials with $r_0=r_{90}$, the main stresses are equal ($\sigma_1 = \sigma_2 = \sigma_b$), as well as the main stain ($\varepsilon_1 + \varepsilon_2 = \varepsilon_b$) and curvature radii ($\rho_1 = \rho_2 = \rho$), which simplifies equation (3) and leads to equation (14) [1,8]:

$$\sigma_b = \frac{P\rho}{2t} \qquad (14)$$

2.3 Materials and Mechanical Characterization

The uniaxial tensile and equibiaxial stretching tests by hydraulic bulge were applied on an Interstitial Free steel (IF) - EEP grade 3 - NBR5915-2[16]. The mechanical properties obtained from the uniaxial tensile test, yield strength (YS), tensile limit (TS), uniform elongation (%ε_u), total elongation (%ε_t), anisotropy

coefficients (r_α) calculated at 20% strain, for the different directions relative to the rolling direction for this steel, are presented in Table 1.

Table 1. Mechanical properties of IF steel - EEP grade 3 relative to different rolling directions - Engineering Stress-Strain.

Direction	YS*	TS*	$\%\varepsilon_u$	$\%\varepsilon_t$	r_α
0º	159	284	27.8	51.3	2.153
45º	161	292	25.9	49.3	1.877
90º	158	282	27.9	52.3	2.595

(*)YS and TS values in (MPa)

Triplicated uniaxial tensile tests were performed for each angular orientation, and the average result values from these tests are presented in Table 1. It was aimed to choose the work-hardening equation that best describes the yield curves obtained. True stress-strain curves plotted up to uniform strain for the IF steel in three different directions are shown in Figure 2.

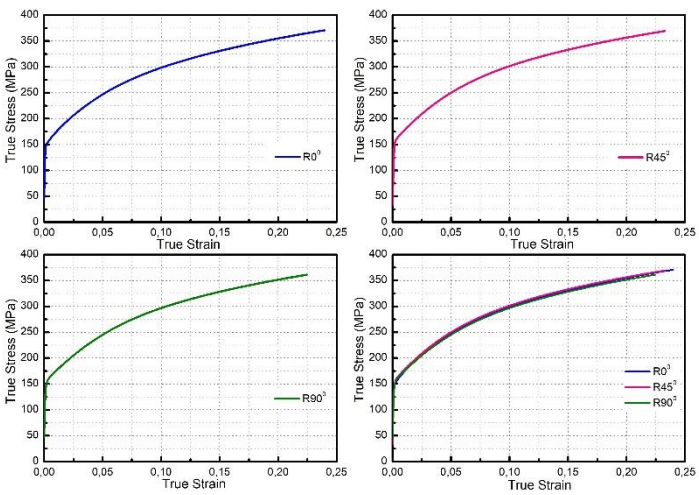

Figure 2. True stress-strain curve for angular orientations with respect to the rolling direction of IF steel sheet.

2.4 Work-hardening equations

Some different work-hardening equations to characterize mechanical behavior of materials considering their behavior as rigid-plastic [17] are shown in Table 2.
The work-hardening equations were tested to the experimental data and the model that best describes the mechanical behavior (strain hardening curve) was chosen by analyzing the quality of adjustments based on a coefficient of determination (R^2) and the root-mean-square of residual percentage (rmsrp) which is described by equation (15) [26]:

$$(rmsrp) = \frac{\sqrt{\sum_N \left(\frac{\chi_{ex}-\chi_{fit}}{\chi_{ex}}\right)^2}}{N} \qquad (15)$$

Where χ_{ex} is the value of the experimental measurement, χ_{fit} is the calculated value of the fitting model to the corresponding experimental point and N is the total of experimental points [26].

Table 2. Work-hardening equations proposed by various authors (chronologically ranked).

Author	Constitutive models
Ludwik (1909) [18]:	$\sigma = \sigma_0 + K \cdot \varepsilon^n$ (16)
Hollomon (1945) [19]:	$\sigma = K \cdot \varepsilon^n$ (17)
Voce (1948) [20]:	$\sigma = \sigma_s - (\sigma_s - \sigma_I) \cdot e^{-\beta\varepsilon}$ (18)
Swift (1952) [21]:	$\sigma = K \cdot (\varepsilon + \varepsilon_0)^{n_s}$ (19)
Ludwigson (1971) [22]:	$\sigma = K_1 \cdot \varepsilon_{pl}^{n_1} + e^{(K_2 + n_2 \cdot \varepsilon_{pl})}$ (20)
Hockett-Sherby (1975) [23]:	$\sigma = \sigma_s - (\sigma_s - \sigma_I) \cdot e^{-a\varepsilon^p}$ (21)
Swift-Voce [24]:	$\sigma = (1-\alpha)[K(\varepsilon + \varepsilon_0)^{n_s}] + \alpha[\sigma_s - (\sigma_s - \sigma_I) \cdot e^{-\beta\varepsilon}]$ (22)
Swift-Hockett/Sherby [25]:	$\sigma = (1-\alpha)[K(\varepsilon + \varepsilon_0)^{n_s}] + \alpha[\sigma_s - (\sigma_s - \sigma_I) \cdot e^{-a\varepsilon^p}]$ (23)

3 RESULTS AND DISCUSSION

The Hill's 48 parameters of equation (6), calculated with values of anisotropy coefficients - r_α (Table 1), follow the condition G + H = 1. This means that the equivalent strain hardening curve can only be compared in the rolling direction, that is direction Ox. Thus, the work-hardening equations adjustments to the uniaxial tensile test data were performed only for samples referring to the rolling direction. Tables 3 and 4 present values calculated by adjustments of the work-hardening equations parameters to the experimental data, with values of (R^2) and (rmsrp).

Table 3. Parameters of work-hardening equations based on data from the IF Steel uniaxial tensile test in the rolling direction.

Model	Parameters			
Ludwik	σ_o = 65.9	k = 496	n=0.33	
Hollomon	k= 531.2	n = 0.25		
Voce	σ_s = 390.8	σ_i = 156.6	β = 9.4	
Swift	k = 549.2	n = 0.27	ε_0 = 0.005	
Ludwig.	k_1 = 540.4	n_1 = 0.26	k_2 = 4.12	n_2 = -183.8
(HS)	σ_s = 438.1	σ_i = 134.5	a = 4.31	p = 0.75
(SV)	k = 549.2	n = 0.27	ε_0 = 0.005	α = 0.637
	σ_s = 390.8	σ_i = 156.6	a = 9.4	p = 1
(SHS)	k = 549.2	n = 0.27	ε_0 = 0.005	α = 0.81
	σ_s = 438.1	σ_i = 134.5	a = 4.31	p = 0.75

All parameter values beginning with σ and k are in MPa. The rmsrp values are in percent. Abbreviations of some models: HS: Hockett-Sherby; SV: Swift-Voce; SHS: Swift-Hockett/Sherby

Table 4. Quality of adjustments for each work-hardening equation based on data from the IF Steel uniaxial tensile test in the rolling direction.

Model	R^2	rmsrp
Ludwik	0.9979	0.0272
Hollomon	0.9962	0.043
Voce	0.9984	0.0217
Swift	0.9988	0.0199
Ludwig.	0.9996	0.01
(HS)	0.9998	0.0068
(SV)	0.9992	0.0161
(SHS)	0.9998	0.0084

By analyzing the values of R^2 (closest to 1) and rmsrp (closest to 0), the work-hardening equation that best describes or represents the strain hardening curve for the evaluated steel is the equation of Hockett-Sherby [23] (Figure 3a). This work-hardening equation agrees with Voce model [20] when p = 1 in equation (21) and the constant a from Hockett-Sherby equation becomes equal to constant β in Voce model, i.e. $a = \beta^p$, where p ranges from 0 to 1. The authors proposed this equation considering that for high levels of plastic strain, the strain hardening curve reaches a steady state, in which will occur a formation of a cell structure of dislocations and in this configuration, there will be a balance between generation (strain hardening) and annihilation (dynamic recovery) of dislocations during the evolution of the strain hardening curve [23].

In Figure 3b it can be seen that the work-hardening equations almost coincide in the true stress-strain domain for the tensile test, so for large strain level there is a divergence between constitutive models. Therefore, the transfer of hydraulic bulge test data by the use of equivalent stresses and strain is of great relevance to confirm which constitutive model is best at large levels of plastic strain.

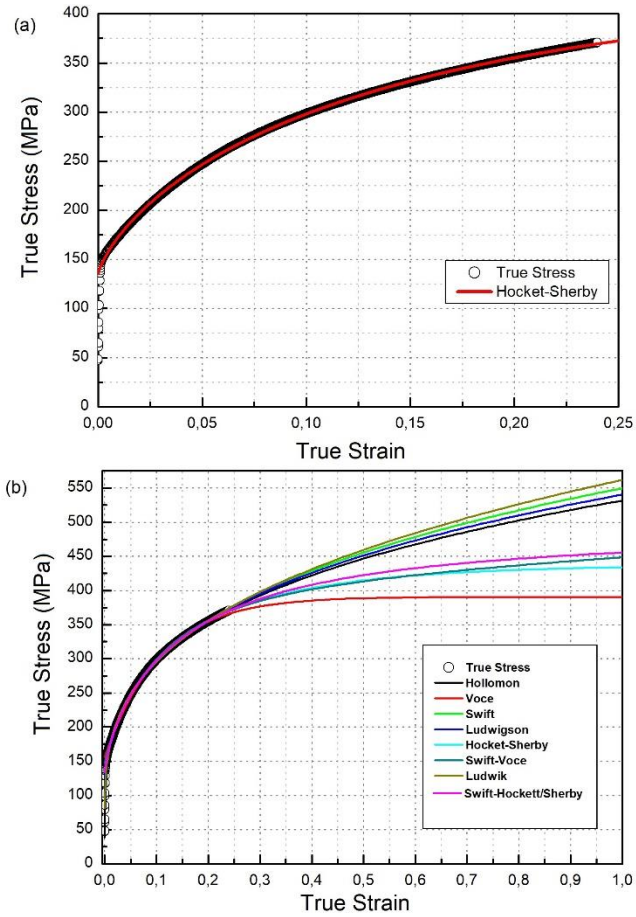

Figure 3. (a) Adjustment of Hockett-Sherby equation to experimental data from the Uniaxial Tensile Test. (b) Comparison between various work-hardening equation with experimental data and strain level.

Although the material is anisotropic with $r_0 \neq r_{45} \neq r_{90}$ (Table 1), it presents close values of mechanical properties (YS, TS, $\%\varepsilon_u$, $\%\varepsilon_t$) in relation to the rolling direction (0º) and transverse (90º), therefore $r_0 \approx r_{90}$. In addition, the stress distribution in the pole

region can be approximated as a rotational symmetry case - equibiaxial stretching - the main stresses (σ_1 and σ_2) can be considered equivalent and equal to the membrane stress ($\sigma_1 \approx \sigma_2 \approx \sigma_b$) [4, 12, 14], then, for this case it is valid to apply equation (14) for generating the symmetrical biaxial strain hardening curve with a good approximation. Equivalent stresses and strains were calculated with equations (10) and (11) respectively. Equations (8) and (9) did not allow a good transfer of symmetrical biaxial to uniaxial stress data for this material under evaluation.

Figure 4 presents the representation of data passage from symmetrical biaxial strain hardening curve to uniaxial stress (Figure 4a). Figure 4b shows the superposition of the uniaxial stress curve with the equivalent strain hardening curve calculated by Hill'48 criterion. This superposition occurs at a point corresponding to the Uniaxial Tensile Strength Limit (TS), generating a combined strain hardening curve, that is, the equibiaxial data used, generates a strain hardening curve extrapolated by the real data. Figure 4b is nothing more than a combined strain hardening curve superimposed on Figure 3b. Although the Hockett-Sherby (HS) model had the best uniaxial strain fit, the extrapolation of the Swift-Hockett / Sherby (SHS) fit appears to be closer to the strain hardening curve for stress values above (TS) (Figure 4b). Again, the constitutive models were adjusted, only now for the combined strain hardening curve, and, by evaluating the values of (R^2) and (rmsrp), two models that best represent the IF steel strain hardening behavior, from YS to major strain levels are the Hockett-Sherby models and the Swift-Hockett-Sherby (SHS) combined model, as shown in Tables 5 and 6. Figure 5a shows a graphical representation of these models adjustments to the combined strain hardening curve data. Both models (HS) and (SHS) led to the best adjustments in comparison to other models, and the same values for (R^2) and (rmsrp). It should be noted that (α) from SHS model, fit on the combined strain hardening curve, was slightly higher than one (due to numerical errors), this means that the portion or weight of the Hockett combined Swift model -Sherby is negligible and the SHS model, for this adjustment, was governed by the (HS) portion (or weight) of this model, since at both low and high strain levels, the Hockett-Sherby model presented the best values of (R^2) and (rmsrp), then among the suggested constitutive models, this one presents the best description and prediction of the plastic behavior for the IF steels under analysis.

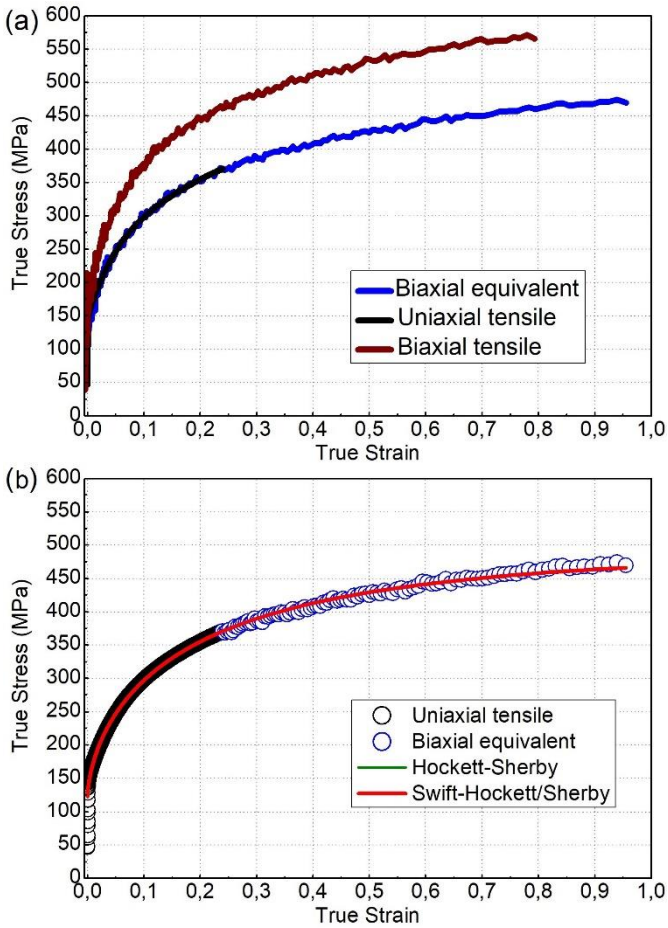

Figure 4. (a) Representation of the equibiaxial stretch data transfer for uniaxial tensile test; (b) Overlapping stress and equivalence data from (TS) point.

In Figure 4b a comparison is made between work-hardening equations

previously identified. It is clear that using only tensile test data, the corresponding (best fit) equations led to less strain hardening for the material in the extrapolation zone. Using the hydraulic bulge test data it is possible to improve prediction and description of the IF steel strain hardening at higher levels of plastic strain.

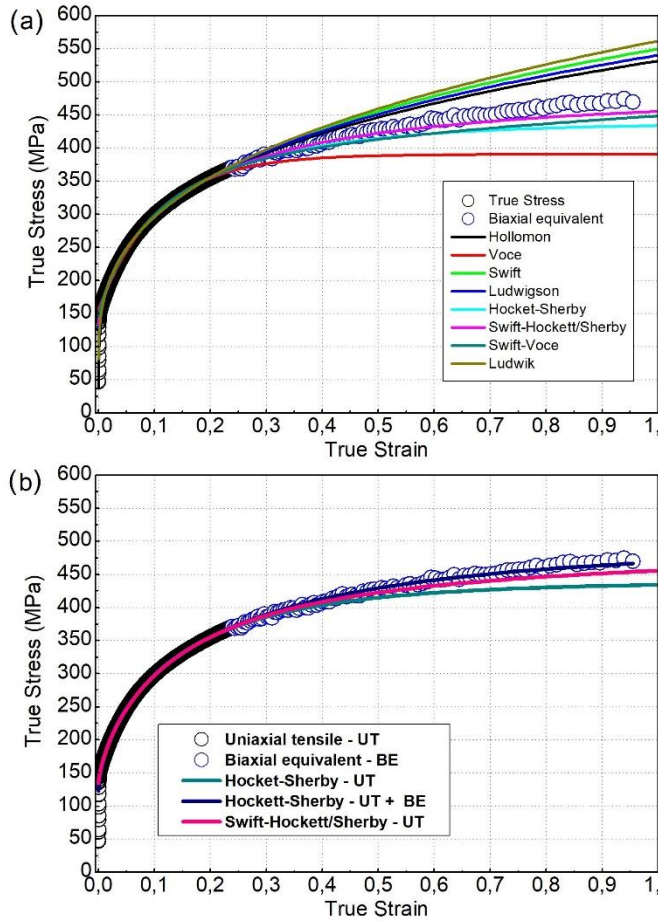

Figure 5. (a) Adjustment of the HS and SHS equations in the combined strain hardening curve; (b) Comparison of the combined strain hardening curve using symmetrical biaxial test data in the selection of the work-hardening equation.

Table 5. Work-hardening equations parameters based on data acquired from combination of the IF Steel uniaxial tensile test data in the rolling direction and the combination with the equivalent Hill stress from the Biaxial test.

Model	Parameters			
Ludwik	σ_0 = -55.25	k = 561	n=0.20	
Hollomon	k= 514.3	n = 0.24		
Voce	σ_s = 438	σ_i = 171	β = 6.1	
Swift	k = 515.2	n = 0.24	ε_0 = 3.65 x 10^{-4}	
Ludwig.	k_1 = 516.5	n_1 = 0.24	k_2 = 4.37	k_1 = 516.5
(HS)	σ_s = 491.95	σ_i = 121.4	a = 2.76	σ_s = 491.95
(SV)	k = 515.2	n = 0.24	ε_0 = 3.65 x 10^{-4}	α = 0.464
	σ_s = 438	σ_i = 171.3	β = 6.1	p = 1
(SHS)	k = 515.2	n = 0.24	ε_0 = 3.65 x 10^{-4}	α = 1.002
	σ_s = 492	σ_i = 171	a = 2.8	p = 0.63

Table 6. Fit quality for each work-hardening equation based on data from combination of the IF Steel uniaxial tensile test data in the rolling direction and the combination with Hill equivalent stress from the Biaxial test.

Model	R^2	rmsrp
Ludwik	0.9922	0.0523
Hollomon	0.9914	0.0479
Voce	0.9892	0.0587
Swift	0.9914	0.0467
Ludwig	0.9925	0.0386
(HS)	0.9994	0.0132
(SV)	0.9981	0.0272
(SHS)	0.9994	0.0132

4 CONCLUSION

In the present study it was possible to generate a strain hardening curve for high levels of plastic strain of an IF steel - EEP grade 3, combining uniaxial tensile and hydraulic bulge test data. This was made possible by transferring data from a equibiaxial strain condition to uniaxial strain using Hill's (1948) yield criterion. This data transfer proved to be an approach with excellent results in reproducing material behavior for high levels of plastic strain, serving as a reference for adjustments of different work-hardening equations. Among the work-hardening equations evaluated, both initial yielding and large straining domains of the stress-strain curve, the Hockett-Sherby, and Swift-Hockett/Sherby equations have proved to be the best describe the plastic behavior for this steel.

Acknowledgement

To FAPES-ArcelorMittal cooperation – Edital nº 05/2018 for the PhD scholarship and project funding granted.

REFERENCES

1 Reis LC, Oliveira MC, Santos AD, Fernandes JV. On the determination of work hardening curve using the bulge test. INT J MECH SCI. 2016; 105: 158-81.

2 Zhao K, Wang L, Chang Y, Yan J. Identification of post-necking stress-strain curve for sheet metals by inverse method. Mech Mater. 2016; 92: 107-118.

3 Slota J, Spisak E. Determination of flow stress by the hydraulic bulge test. Metallurgy. 2008; 48(1): 13-17.

4 Campos H, Santos AD, Amaral R. Experimental and analytical evaluation of the stress-strain curves of AA5754-T4 and AA6061-T6 by hydraulic bulge test. Ciência & Tecnologia dos Materiais. 2017; 29: 244-8.

5 ASTM A370-18. Standard test methods and definitions for mechanical testing of steel products. American Society for Testing and Materials, feb. 27, 2019.

6 Maummer K, Billur E, Cora ÖN. An experimental study on the comparative assessment of hydraulic bulge test analysis methods. Mater Des. 2011; 32: 272-81.

7 Rana R, Singh SB, Bleck W, Mohanty ON. Biaxial stretching behaviour of a copper-alloyed insterstitial-free steel by bulge test. Metall Mater Trans A. 2010; 41A: 1483-92.

8 Reis LC, Prates PA, Oliveira MC, Santos AD, Fernandes JV. Anisotropy and plastic flow in the circular bulge test. Int J Mech Sci. 2018; 128-129: 70-93.

9 Mulder J, Vegter H, Aretz H, Keller S, van den Boogaard AH. Accurate determination of flow curves using the bulge test with optical measuring systems. J Mater Process Tech. 2015; 226: 169-187.

10 Hill R. A theory of plastic bulging of a metal diaphragm by lateral pressure. Philos Mag Ser. 1950; 41(322):1133-42.

11 Pham QT, Oh Hwan S, Park KC, Kim YS. Material modeling of pure titanium sheet and its application to bulge test simulation. Procedia Manuf. 2018; 15: 1886-92.

12 Cardoso RPR, Adetoro OB. A generalization of the Hill's quadratic yield function for planar plastic anisotropy to consider loading direction. Int J Mech Sci. 2017; 128-129: 253-68.

13 Banabic D. Sheet metal forming processes – Constitutive modelling and numerical simulation. Germany: Springer Berlin Heidelberg; 2010.

14 Amaral R, Santos AD, Lopes AB, Souza J. Determinação da curva de encruamento usando o ensaio uniaxial de tração e o ensaio hidráulico de expansão biaxial-aplicação aos aços DP500, DP600 e DP780. In: Congresso de Métodos Numéricos em Engenharia; 2015 29 Jun- Jul 2; Lisboa, Portugal. Lisboa: APMTAC.

15 Rees DWA. Plastic flow in the elliptical bulge test. Int J Mech Sci. 1995; 37(4): 373-89.

16 5915-2, ABNT NBR. Chapas e bobinas de aços laminadas a frio, Parte 2: Aços para estampagem – Brasil, 2013. Técnicas, ABNT-Associação Brasileira de Normas.

17 Marcianiak Z, Duncan JL, Hu SL. Mechanics of sheet metal forming. Oxford: Butterworth-Heinemann; 2002.

18 Ludwik P. Elemente der Technologischen Mechanic. Verl. Julius Springer; 1909.

19 Hollomon JH. Tensile deformation. Trans. AIME. 1945; 162:268-90.

20 Voce E. The relationship between stress and strain for homogeneous

deformation. J Inst Met. 1948; 74: 537-62.

21 Swift WH. Plastic instability under plane stress. J Mech Phys Solids. 1952; 1:1-18.

22 Ludwigson DC. Modified stress-strain relation for FCC metals and alloys. Metall Trans. 1971; 2: 2825-28.

23 Hockett JE, Sherby OD. Large strain deformation of polycrystalline metals at low homologous temperatures. J Mech Phys Solids. 1975; 23 (2): 87-98.

24 Kessler L, Gerlach J. The impact of materials testing strategies on the determination and calibration of different FEM material models. In: Proceeding of IDDRG 2006, Leca do Balio, Portugal, 113-120.

25 Autoform Engineering GmbH, Autoform Plus R 3.1 User'sManual.

26 Dimatteo A, Colla V, Lovicu G, Valentini R. Strain hardening behavior prediction model for automotive high strength multiphase steels. Steel Res Int. 2015; 86: 1574-82.